PARALINEAR OXIDATION OF SILICON NITRIDE IN A WATER VAPOR/OXYGEN ENVIRONMENT

Dennis S. Fox*, Elizabeth J. Opila*†, QuynhGiao N. Nguyen*,
Donald L. Humphrey‡ and Susan M. Lewton§

National Aeronautics and Space Administration
John H. Glenn Research Center at Lewis Field
Cleveland, OH 44135

Three silicon nitride materials were exposed to dry oxygen flowing at 0.44 cm/s at temperatures between 1200° and 1400°C. Reaction kinetics were measured with a continuously recording microbalance. Parabolic kinetics were observed. When the same materials were exposed to a 50% H_2O - 50% O_2 gas mixture flowing at 4.4 cm/s, all three types exhibited paralinear kinetics. The material is oxidized by water vapor to form solid silica. The protective silica is in turn volatilized by water vapor to form primarily gaseous $Si(OH)_4$. Nonlinear least squares analysis and a paralinear kinetic model were used to determine both parabolic and linear rate constants from the kinetic data. Volatilization of the protective silica scale can result in accelerated consumption of Si_3N_4. Recession rates under conditions more representative of actual combustors are compared to the furnace data.

* Member, American Ceramic Society
† Cleveland State University Resident Research Associate at NASA GRC
‡ QSS Group Inc., Brookpark, OH; Research Technician at NASA GRC
§ Work performed while a NASA/Ohio Aerospace Institute summer intern; currently at Purdue University, Department of Chemical Engineering, West Lafayette, IN

This report is a preprint of an article submitted to a journal for publication. Because of changes that may be made before formal publication, this preprint is made available with the understanding that it will not be cited or reproduced without the permission of the author.

I. Introduction

The high strength, high temperature capability and low density of silicon-based ceramics such as silicon nitride (Si_3N_4) and silicon carbide (SiC) make them candidate materials for application in the hostile environments of advanced aeropropulsion engines. The oxidation behavior of Si_3N_4 has been studied in great detail, as reviewed in Ref. 1. When Si_3N_4 reacts with dry oxygen at 1200°-1500°C, silica (SiO_2) is formed:

$$Si_3N_4 + 3\ O_2(g) = 3\ SiO_2(s) + 2\ N_2(g) \qquad [1]$$

The exceptional oxidation resistance of Si_3N_4 in dry oxygen results from the slow diffusion of oxygen through the solid surface layer of silica and a thin inner layer of silicon oxynitride.[2-3] In this environment, the material exhibits parabolic kinetics that can be described by:

$$x^2 = k_p \times t \qquad [2]$$

where x is the silica thickness in microns (μm), t is time and k_p is the parabolic rate constant ($\mu m^2/h$). In thermogravimetric oxidation experiments wherein sample weight is measured as a function of time, x is weight gain (mg/cm^2) and k_p is in (mg^2/cm^4 h).

If silicon based ceramics are to be used in combustion applications, their behavior under fuel-lean conditions must be determined. Jacobson has calculated equilibrium products resulting from fuel-lean combustion of Jet A aviation fuel ($CH_{1.9185}$).[1] The products include O_2, H_2O, CO_2, and N_2. Independent of the fuel-to-air ratio, the amount

of water vapor remains nearly constant at approximately 10%. In such an environment, the primary oxidant is water vapor:[4]

$$Si_3N_4(s) + 6\ H_2O(g) = 3\ SiO_2(s) + 2\ N_2(g) + 6\ H_2(g) \qquad [3]$$

$$SiC(s) + 3\ H_2O(g) = SiO_2(s) + CO(g) + 3\ H_2(g) \qquad [4]$$

Others have recognized the need to study the oxidation of silicon nitride in water-vapor containing environments.[5-11] However, none have measured kinetics continuously. Singhal[5] studied the kinetics of hot-pressed Si_3N_4 containing Mg from 1200° to 1400°C in dry oxygen and in oxygen containing 3.3% water. The kinetics were higher in the wet oxygen, attributed to either the diffusion of OH^- ions through the surface silica or to a slight viscosity change of the oxide, altering the diffusion rate of the additives. Mayer and Riley[6] studied the oxidation kinetics of reaction-bonded silicon nitride in atmospheric air containing 1.5% H_2O from 800° to 1200°C. The oxidation rates were the same as in dry air. Sato, *et al.*[7] oxidized Si_3N_4 with Al and Y additions in both dry air and wet nitrogen at 1100° to 1350°C, in 1.5 - 20% water vapor. The rates were the same both dry and wet, indicating that the diffusion rate of water vapor as OH^- and O^{2-} through the silica did not control the oxidation rate, rather the diffusion of Y^{3+} through silica controlled the rate of oxidation.

Maeda, *et al.*[8] exposed hot-pressed Si_3N_4 containing Y and Al in air containing 0 to 40% water vapor at 1300°C. Weight gain increased with increasing water vapor content. Si_3N_4 kinetics were measured (not continuously) in 20% H_2O up to 360 h.

Parabolic oxidation kinetics were observed at a slightly faster rate than in dry oxygen, with diffusion of oxidants through the oxide occurring. Maeda, *et al.*[9] also looked at the oxidation resistance of five different silicon nitrides with various additives at 1300°C in flowing dry and wet air up to 40% water vapor. Again, a linear relationship was observed between water vapor content and weight gain was noted, though kinetics were not measured in the study.

Choi, *et. al.*[10] studied the effect of dry and wet oxygen, including steam, on the oxidation of chemical vapor deposited (CVD) Si_3N_4 for ~10 h at 1000° to 1300°C. Weight change was measured at various times. Parabolic behavior was observed, and water vapor was found to be the major oxidant. Proverbio, *et al.*[11] studied the influence of 0.1%, 3.2% and 50% water vapor on the oxidation of Si_3N_4 containing Al and Mg at 1200°C. Weight gain increased as a function of increasing water vapor content. It was felt that devitrification of the oxide layer promoted the oxidation rate and caused an increase of porosity cracks, bubbles and blowholes.

CVD silicon carbide in water vapor

Work was previously conducted at the Glenn Research Center (GRC) on the effects of water vapor on the oxidation of silicon carbide. Opila found that that CVD SiC exhibits parabolic oxidation kinetics in 10% H_2O - 90% O_2 environment at 100 kPa (1 atm) total pressure.[12] Gas turbines, however, operate at higher than atmospheric pressure. In an engine operating at 500 kPa (5 atm), the partial pressure of water vapor would be 50 kPa (0.5 atm). Opila and Hann found that in a 50% H_2O - 50% O_2 environment at 100 kPa (1 atm) total pressure, CVD SiC exhibits *paralinear* behavior

(Fig. 1).[13] The kinetics result from the simultaneous oxidation of SiC to form silica and the volatilization of the silica by reaction with the water vapor. In the same study, a linear weight loss was observed for a fused quartz coupon exposed to 50% H_2O - 50% O_2 (Fig. 1). Preoxidized SiC exhibited similar behavior to the fused quartz.

The question then arose as to the identity of the volatile species from the SiO_2 - H_2O reaction. Previous studies conducted under various conditions suggested a number of possible species including $Si(OH)_4$, $SiO(OH)$, $SiO(OH)_2$, and $Si_2O(OH)_6$.[14-16] A high pressure sampling system/quadrupole mass spectrometer at GRC was used to determine the products of the reaction of fused quartz frit exposed to water-saturated oxygen at 1300°C.[17] The primary volatile species was found to be $Si(OH)_4$, with $SiO(OH)_2$ also observed:

$$SiO_2(s) + 2\ H_2O(g) = Si(OH)_4(g) \qquad [5]$$

$$SiO_2(s) + H_2O(g) = SiO(OH)_2(g) \qquad [6]$$

Paralinear Kinetics

Paralinear oxide scale thickness kinetics have been expressed mathematically by Tedmon for oxidation of Fe-Cr alloys.[18] In that system, parabolic oxidation results in solid Cr_2O_3 formation, with concurrent reaction of the oxide with O_2 to form volatile $CrO_3(g)$. Tedmon's expression incorporates the parabolic and linear rate constants in terms of oxide thickness (k_p' in $\mu m^2/h$ and k_l' in $\mu m/h$). It can also be used to describe the paralinear kinetics resulting from the changes in the SiO_2 thickness that occurs in

the SiC-H_2O-O_2 system[13], as well as the Si_3N_4-H_2O-O_2 system. At long exposure times, a limiting oxide thickness is reached that is equal to $k_p'/2k_l'$. However, even before reaching the limiting oxide thickness, a recession rate of the underlying Si_3N_4 can be approximated using only the linear SiO_2 volatility rate.

Paralinear kinetics of SiC have also been followed using thermogravimetric analysis.[13, 19] In this case, weight change due to both silica growth and subsequent volatilization is measured, rather than oxide thickness. Using the appropriate molecular weights, the kinetics can be described by:

$$t = \frac{\alpha^2 k_p}{2(k_l)^2}\left[\frac{-2k_l \Delta w_1}{\alpha k_p} - \ln\left(1 - \frac{2k_l \Delta w_1}{\alpha k_p}\right)\right] \qquad (7)$$

$$\Delta w_2 = -\beta k_l t \qquad (8)$$

For the SiC case, $\alpha = MW_{SiO2} / (MW_{O2} - MW_C)$ and $\beta = MW_{SiC} / MW_{SiO2}$ (where MW is molecular weight), k_p is the oxidation parabolic rate constant in units of specific weight squared versus time (mg^2/cm^4 h), k_l is the volatilization linear rate constant (mg/cm^2 h), Δw_1 = weight gain from silica growth, and Δw_2 = weight loss from silica volatilization. The paralinear model used herein was developed for SiC. When the molecular weights of Si_3N_4 and N_2 are inserted into this model ($\alpha = MW_{SiO2} / [MW_{O2} - 2/3\ MW_{N2}]$ and $\beta = MW_{SiN1.3} / MW_{SiO2}$), it closely approximates the paralinear kinetics occurring in the Si_3N_4/H_2O vapor system.

The objective of this paper is to determine the oxidation behavior of three Si_3N_4 materials in both dry oxygen and in 50% H_2O - 50% O_2 from 1200° to 1400°C. Nonlinear least squares analysis and a paralinear kinetic model described in Ref. 13 are used to determine both k_p and k_l from the continuously measured kinetic data during the water vapor exposures. Recession of the substrate under the furnace conditions is estimated and compared to previous results for very pure silicon carbide. Silicon nitride recession rates from the furnace data are extrapolated to more realistic, high velocity conditions. These are compared to experimental results from a high-pressure burner rig.

II. Experimental Procedure

The materials used in this study are described in Table I. The α-Si_3N_4 is produced via chemical vapor deposition. SN282 is a high strength β-Si_3N_4 with an improved oxidation resistant grain boundary phase developed for gas turbine applications. The AS800 material is an in-situ reinforced β-Si_3N_4 developed to enable a new generation of power systems. A rare earth-based sintering system is used in production of the material, resulting in an apatite grain boundary phase.

Specimens were cleaned using a detergent solution, distilled water, acetone and alcohol. Sample weight was measured on an analytical pan balance (± 0.01 mg) before exposure, as well as at the end of the experiment. Oxidation experiments were conducted in a vertical tube furnace at three temperatures: 1200°, 1300° and 1400°C (all ±10°C). Fused quartz furnace tubes were used (Quartz Scientific, Fairport Harbor, OH).

The oxidation kinetics were followed using thermogravimetric analysis (TGA). Weight change was continuously monitored with a recording microbalance (C-1000, Cahn Instruments, Cerritos, CA). Samples were suspended on sapphire hangers inside a 2.5-cm ID vertical furnace tube. Initial experiments were conducted with dry oxygen flowing at 0.44 cm/sec in a fused quartz tube. A minimum of three samples of each composition was run in dry O_2 for 100 hours at each of the three test temperatures. Specific weight gain (mg/cm^2) was measured as a function of time, and the parabolic rate constant (k_p in mg^2/cm^4 h) was determined.

For the subsequent water vapor-oxygen tests, an experimental apparatus based on a design by Belton and Richardson[20] was used. A schematic is found in Ref. 12. The reaction gas was introduced at the bottom of the fused quartz furnace tube. Water was added to the oxygen by first over-saturating the gas with deionized water. A high flow rate of 4.4 cm/sec was needed to enable saturation of the gas stream. The gas then passed through a glass bead-filled saturator immersed in a water bath held at 81.7°C. The resulting oxygen stream was saturated with 50% water vapor. A counter flow of oxygen through the top of the TGA apparatus was used to keep water from condensing on the microbalance and hangwire. A minimum of two samples of each Si_3N_4 type was run at each of the three test temperatures. Weight change versus time was continuously measured during the 100 hours.

The surface oxide was characterized by X-ray diffraction (XRD) following TGA exposure of the as-received samples. Oxide morphologies were then studied using a scanning electron microscope (SEM; JEOL JSM-840A, Tokyo, Japan). Polished cross-sections of selected samples were prepared in order to measure the silica scale

thickness. One of the ~2.5 x 0.3 cm edges was polished to a 15 micron finish for observation by SEM and entailed oxide thickness measurements every 1 mm along the 25 mm edge. The average thickness for each selected sample is reported. A National Bureau of Standards calibration standard was used to establish the appropriate correction factor for reporting thickness. It was determined that the measured thickness was approximately 5.3% greater than the true thickness.

III. Results

(1) Dry oxygen

Thermogravimetric analysis results for a single run of each of the three Si_3N_4 materials at 1300°C in dry oxygen flowing at 0.44 cm/s are shown in Fig. 2. The kinetics exhibited parabolic behavior. The weight gain continues as a function of time, though the rate slows as the silica scale increases in thickness (Eq. 2).

The measured kinetic reaction rates for AS800 at the intermediate 1300°C temperature were quite scattered (Fig. 3). At this temperature, samples from three different lots of material were used. Depending on the lot, pre-test specimen color ranged from beige to black (note that C is a minor additive – Table I). A 95% confidence interval was therefore determined for all the data at all three temperatures because of this 1300°C scatter.[21] The resulting band is plotted as dashed lines in Fig. 3. The four 1300°C data points within the band were then used for activation energy calculations. The measured parabolic rate constants for the three materials in dry oxygen are listed in Table II along with the calculated activation energies for the oxide formation.

After TGA exposure, the surface oxide was characterized by X-ray diffraction (Table III). The oxide on the 1200°C CVD Si_3N_4 sample was amorphous. In all other cases, the major crystalline phase was α-cristobalite. Representative photos after 1400°C exposure are shown in Fig. 4. The surface morphology of a typical silica scale shows cracks that are due to the phase transformation from beta-to-alpha cristobalite on cooling. The oxide formed on SN282 also contained $Lu_2Si_2O_7$ and possibly Lu_2SiO_5, and the oxide formed on AS800 also possibly contained Y_2O_3.

The silica scale thickness from polished cross sections was measured using the SEM. The results of the oxide measurements made on single samples of all three materials after exposure in dry oxygen are listed in Table IV. The oxides grown on CVD and SN282 at 1200°C were too thin to measure by this technique.

(2) 50% H_2O - 50% O_2

In 50% H_2O - 50% O_2 flowing at 4.4 cm/sec, *paralinear* kinetics are observed for all three Si_3N_4 materials (Figs. 5-7). In comparing the weight change plots in O_2 and H_2O/O_2, the difference between paralinear and parabolic behavior is apparent. Though CVD Si_3N_4 initially gains weight in the water-vapor environment, the kinetics begin to change to a linear weight loss after ~20 h. This is due to the volatilization of the silica scale that occurs concurrently with the oxidation. The noise in the kinetic curves is due to the high sensitivity of the microbalance scale required to measure the very small weight changes (~0.1 mg/cm^2), and the high 4.4 cm/sec flow rate.

Once the paralinear nature of the reaction in 50% H_2O - 50% O_2 is established, the parabolic oxidation rate constants (k_p) and the linear volatility rate constants (k_l) can be

determined. The fit of the model to the data is shown as the solid line in Figs. 5-7. This is the sum of the weight changes from both the oxidation and volatilization reactions, as determined by the non-linear least-squares analysis of the data. The rate constants determined from the analysis (k_p in mg^2/cm^4 h, and k_l in mg/cm^2 h) are noted on each graph. After 40-60 h, an overall weight loss is observed. In comparison, CVD SiC in 50% H_2O - 50% O_2 still shows an overall weight gain after 100 h (Fig. 1). This difference is attributed to the lower k_p values for Si_3N_4 compared to SiC. Table V summarizes the *parabolic* rate constants, and Table VI the *linear* rate constants, for the three Si_3N_4 materials from the paralinear data in 50% H_2O-50% O_2.

The volatility fluxes determined experimentally for the three Si_3N_4 materials are plotted in an Arrhenius diagram in Fig. 8 (open circles). The activation energy (E_a) from a fit of all the data points (solid line) is calculated to be 36 ± 86 kJ/mol (95% confidence interval), which indicates little temperature dependence. As after the dry oxygen exposure, the major crystalline oxide phase after 50% H_2O-50% O_2 exposure was α-cristobalite (Table III). The oxide formed on SN282 contained $Lu_2Si_2O_7$. The AS800 material exhibited peaks tentatively identified as $La_2Si_2O_7$ and Y_2O_3. Representative photos after 1400°C exposures are shown in Fig. 9. Oxide thickness measurements, for single specimens after exposure in 50% H_2O - 50% O_2, are listed in Table IV. The CVD oxides grown at 1200° and 1300°C were too thin to measure by this technique, as was that on SN282 at 1200°C.

IV. Discussion

(1) Parabolic behavior in dry oxygen

Parabolic rate constants for the three materials in dry oxygen as a function of reciprocal temperature are shown in Fig. 10. The pure CVD Si_3N_4 is the most oxidation resistant, with an activation energy of 227 ± 44 kJ/mol. Regarding the lanthanide (rare-earth)-containing Si_3N_4, the AS800 material (135 ± 31 kJ/mol) is less oxidation resistant than the SN282 (204 ± 79 kJ/mol). X-ray diffraction of the surface oxide shows α-cristobalite forms on both materials. However, the additional formation of $Lu_2Si_2O_7$ in the SN282 oxide plays a beneficial role.

Others have studied the oxidation of Si_3N_4 containing lanthanide rare-earth elements (which can also include Y and Sc). These previous results show there is no distinct correlation between rare-earth atomic element number and oxidation resistance. Mieskowski and Sanders[22] observed that Y-containing Si_3N_4 had the lowest oxidation rate in air at 1370°C, followed in order by La, Sm and Ce-containing material. Cinibulk and Thomas[23] found that Er-containing Si_3N_4 had the lowest oxidation rate in laboratory air at 1400°C, followed in order by Yb, Dy, Y, Gd and Sm. Crystallites of the form $Re_2Si_2O_7$ were observed. Choi, et al.[24] conducted oxidation studies in laboratory air at 1400°C and noted Er-containing Si_3N_4 had the lowest oxidation rate, followed in order by Y, Yb, and La.

(2) Paralinear behavior in 50% water vapor

The paralinear nature of the reaction kinetics of Si_3N_4 with 50% H_2O - 50% O_2 is obvious from the kinetic curves. Additional evidence is provided by comparison of calculated weight change, from SEM oxide measurements, with that actually measured. For oxidation alone, the oxide thickness (x) and weight gain (mg/cm^2) are related by the expression

$$x = 19.4 \times \Delta wt \qquad (9)$$

when cristobalite is formed.[25] Using the measured oxide thickness, one calculates positive weight gains for each of the materials (Table VII). However, there is a clear discrepancy when the samples are weighed on the analytical pan balance. Actual weight gains were much less than that calculated, and in two cases overall weight losses were observed. The AS800 sample at 1400°C doesn't follow this trend, likely due to formation of a low-viscosity scale at this temperature. It is therefore evident that, although an oxide is continually being formed, volatilization of the silica by H_2O is also occurring. This results in recession of the underlying Si_3N_4 substrate and subsequent weight loss.

The k_l values for CVD Si_3N_4, AS800 Si_3N_4 and CVD SiC[13] under the same conditions (Table VI) are comparable. This provides evidence that any additional protection provided by silicon oxynitride for CVD Si_3N_4 in dry oxygen is not active in a 50% H_2O - 50% O_2 environment. This also demonstrates that the paralinear equations described herein can be applied to other silica formers. The k_l values for SN282 Si_3N_4

are slightly lower than those for the other materials. This is attributed to the formation of $Lu_2Si_2O_7$ in the oxide, resulting in a lower Si activity. When the Table VI data is plotted on an Arrhenius diagram, only a slight temperature dependence across the range of 1200°-1400°C is observed for all four materials.

The surface morphologies of the silicon nitride materials after 100 h at 1400°C in 50% H_2O - 50% O_2 are found in Fig. 9. The cracks in the oxide are formed from the transformation of beta-to-alpha cristobalite on cooling. XRD of CVD Si_3N_4 at 1200°C shows the oxide to be amorphous. Alpha-cristobalite is observed after 1300° and 1400°C exposures. In comparison, Choi, *et.al.*[10] observed amorphous SiO_2 after steam exposure of CVD Si_3N_4 at 1000° to 1300°C for 10 hours.

As discussed in the Introduction, others have previously conducted water vapor studies of additive-containing Si_3N_4. After exposure, various crystallites were observed. Sato, *et al.*[7] oxidized Si_3N_4 with Al and Y in wet nitrogen. The oxide film consisted of α-cristobalite, $Y_4Al_2O_7$, and $Y_2Si_2O_9$. Maeda, *et al.*[8] exposed hot pressed Si_3N_4 containing Y and Al in water vapor/air. $Y_2Si_2O_9$ crystals were observed on the cristobalite surface oxide, as were cracks, bubbles and blowholes. Proverbio, *et al.*[11] studied the influence of water vapor on the oxidation of Si_3N_4 containing Al and Mg at 1200°C. Weight gain increased as a function of increasing water vapor content. It was felt that devitrification of the oxide layer promoted the oxidation rate and caused an increase of porosity cracks, bubbles and blowholes. Cristobalite, enstatite and clinoestatite were observed.

In the present study, after exposure of the Lu-containing SN282, alpha-cristobalite and $Lu_2Si_2O_7$ were observed by XRD. The AS800 oxides were identified as α-

cristobalite, and tentatively Y_2O_3 and $La_2Si_2O_7$. No formation of bubbles and blowholes was observed in the oxide after water vapor exposure for any of the three materials, as has been found in SiC under similar conditions.[26] This could be due to the fact that the Si_3N_4 oxides are thinner (because of lower oxidation rates) or they may be of lower viscosity.

The measured k_p values in 50-50 water-oxygen in this study (Table V) are one to two orders of magnitude higher than those measured in dry oxygen (Table II). This demonstrates that the oxidation rate is not controlled by transport of additives outward, since the rates are sensitive to the oxidant. It is well known that water vapor enhances the oxidation rate in both SiC[26] and Si.[27] The k_p values determined from the paralinear data are sensitive to the choice of time zero, and are therefore less accurate than the k_l values. It should be emphasized here that the k_l values are the more essential parameter derived from the paralinear modeling. The recession calculations described below are based on the silica volatilization kinetics.

(3) Linear weight loss rates

The measured flux (Table VI) can be compared to the calculated flux.[28] The appropriate relation for the flux of the volatile species from a flat plate through a gaseous boundary layer under laminar flow conditions is:[29]

$$J = 0.664 \left(\frac{\rho' v L}{\eta}\right)^{1/2} \left(\frac{\eta}{\rho' D}\right)^{1/3} \frac{D\rho}{L} \qquad (10)$$

where ρ is the concentration of the major gas species and η is the gas viscosity. Gas concentration is calculated using the ideal gas law. Hashimoto has measured thermodynamic data for $Si(OH)_4$.[15] Krikorian[30] and Allendorf, *et al.*[31] have calculated data for the Si-O-H system. Using these data sets in a free energy minimization code (Chemsage, GTT Technologies, Sweden), one can calculate vapor pressures of Si-O-H species. For these calculations, SiO_2 (cristobalite) plus an initial gas composition of 50% H_2O - 50% O_2 was used. The calculated vapor pressures of Si-O-H species are then used in the boundary layer diffusion model, and Si_3N_4 mass loss rates are determined. The best agreement with the experimental data is for $Si(OH)_4$ as the primary volatile species (E_a = 69 kJ/mol). The calculated mass loss rate is shown in Fig. 8 as the dotted line. When including Krikorian's data for $SiO(OH)_2$, the calculated mass loss rates are ~10X larger than those measured experimentally. The activation energy is also high at 205 kJ/mol. Thus the magnitude and temperature dependence of the measured flux is best described by $Si(OH)_4$ formation.

(4) Material recession and life prediction

Many combustion applications require components to be used for thousands of hours. If the component is fashioned from Si_3N_4 and is operating in a fuel-lean environment, some concerns need to be addressed. The linear rate constant given in terms of weight loss can be directly related to recession of the substrate. After an initial period, the rate of silica volatilization is equivalent to the rate at which silica is formed. Because the *substrate* is consumed to form the silica at the same rate that the silica is being volatilized, *substrate recession* can be estimated using k_l. A target recession limit

used by this laboratory for certain applications is 2.5×10^{-6} cm/h (10 mils/10,000 h). For CVD Si_3N_4 with a density of 3.2 g/cm^3, this equates to a maximum allowable k_l of 8×10^{-3} mg/cm^2 h. The values listed in Table VI are slightly lower than this allowable limit.

The TGA experiments provide an acceptable simulation of the temperature and water vapor partial pressures found in an engine environment. However, engines operate at high total pressures. The flow rates encountered in a turbine engine are also much higher than the 4.4 cm/s used in the TGA experiments. At higher flow rates and system pressures, flux estimates can be made by using a simplified form of Eq (10). For this approximation, the diffusion coefficient (D) is proportional to $1/P_{TOTAL}$, and ρ is proportional to P_{TOTAL}. Assuming that $Si(OH)_4(g)$ is the only volatile species and is formed via reaction [5], then ρ is proportional to $P_{Si(OH)4}$:

$$k_l \propto \frac{v^{1/2} \times P(H_2O)^2}{(P_{TOTAL})^{1/2}} \qquad (11)$$

For example, under the combustion conditions of 1200°C (2200°F), gas velocity (v) of 21 m/sec (63 ft/sec), P_{TOTAL} is 600 kPa (6 atm), and $P(H_2O)$ = 60 kPa (0.6 atm), the calculated k_l is ~13 times the furnace k_l. Using AS800 Si_3N_4 as an example (3.32 g/cm^3), with its average k_l of 5.9 x 10^{-3} mg/cm^2 h from the 1200°C furnace data, the material's recession rate would be 2.28×10^{-5} cm/h (91 mil/10,000 h). This is an order of magnitude higher than the acceptable limit. This increase is due to much higher combustion gas velocity ($v^{1/2}$ component in Eq. 11).

The conditions described in the last paragraph were those *actually used* for high-pressure burner rig (HPBR) testing of CVD and AS800 Si_3N_4 under fuel-lean conditions at GRC.[32] Additional HPBR tests of SN282 have since been conducted. The rig itself is described in detail in Ref. 33. Weight change and sample thickness measurements were made every 8 -16 h. As expected, all three materials exhibit paralinear behavior. Both the parabolic and linear rate constants were obtained from the kinetic data. For an AS800 sample exposed at 1230°C, k_l was 7.5 x 10^{-2} mg/cm^2 h, which correlates to a recession rate of 2.26 $\times$ 10^{-5} cm/h (89 mil/10,000 h) – virtually the same rate predicted from the furnace results at 1200°C. A comparison of weight loss of all three forms of Si_3N_4 under standard fuel-lean conditions in the HPBR is shown in Fig. 11. As in the TGA experiments, SN282 Si_3N_4 exhibits the lowest recession rates. This is likely due to formation of $Lu_2Si_2O_7$ in the surface oxide, which results in a reduction of silica volatility. It should be mentioned that the flow in the burner rig is complicated with respect to laminar or turbulent flow conditions. Turbulent flow would increase the flux and corresponding recession rate.

It is clear that silicon nitride linear weight loss and surface recession result from silica scale volatility as seen in the TGA experiments as well as in more realistic burner rig tests. A considerable amount of substrate recession can occur after only hundreds of hours of exposure in the latter. Those proposing to use Si_3N_4 components in a fuel-lean combustion application such as a turbine engine must therefore be aware that silica volatility can occur and will result in loss of component cross sectional area.

V. Summary and Conclusions

Silicon nitride exhibits parabolic kinetics when exposed in a dry oxygen environment flowing at 0.4 cm/s in a fused quartz furnace tube at 1200° to 1400°C. However, the material exhibits paralinear kinetics when exposed in a 50 H_2O - 50% O_2 gas mixture flowing at 4.4 cm/s. The material is oxidized by water vapor to form solid silica. The protective silica is in turn volatilized by water vapor to form primarily gaseous $Si(OH)_4$. At long exposure times, the kinetics can be approximated by the linear rate constants from the volatilization reaction. As a result of this exposure, accelerated consumption of Si_3N_4 occurs.

Recession rates determined from the furnace experiments can be used to estimate substrate recession under more realistic combustion conditions. Component recession, predicted from TGA results and observed under fuel-lean combustion conditions (T=1200°C, P = 6 atm, V_{gas} = 20 m/s), is on the order of 2.5 x 10^{-5} cm/h (1 mil/100 h). Engine designers must be aware of the possible rapid recession of Si_3N_4 under turbine engine combustion conditions. Performance of turbine vanes or blades, with their thin trailing edges, would be especially at risk from this mechanism of degradation.

Acknowledgment: The authors would like to offer their sincere thanks to both Ralph G. Garlick and Dereck F. Johnson of the NASA Glenn Research Center at Lewis Field for the X-ray diffraction results and chemical analysis of the starting materials, respectively.

REFERENCES

[1]N. S. Jacobson, "Corrosion of Silicon-Based Ceramics in Combustion Environments," *J. Am. Ceram. Soc.*, **76** [1] 3-28 (1993).

[2]H. Du, R. E. Tressler, K. E. Spear, and C. G. Pantano, "Oxidation Studies of Crystalline CVD Silicon Nitride," *J. Electrochem. Soc.*, **136** [5] 1527-1536 (1989).

[3]L. U. J. T. Ogbuji and E. J. Opila, "A Comparison of the Oxidation Kinetics of SiC and Si_3N_4," *J. Electrochem. Soc.*, **142** [3] 925-30 (1995).

[4]E. J. Opila and Q. N. Nguyen, "The Oxidation of CVD Silicon Carbide in Carbon Dioxide," *J. Am. Ceram. Soc.*, **81** [7] 1949-52 (1998).

[5]S. C. Singhal, "Effect of Water Vapor on the Oxidation of Hot-Pressed Silicon Nitride and Silicon Carbide," *J. Am. Ceram. Soc.*, **59** [1-2] 81-82 (1976).

[6]M. I. Mayer and F. L. Riley, "Sodium-Assisted Oxidation of Reaction-Bonded Silicon Nitride," *J. Mater. Sci.*, **13** 1319-28 (1978).

[7]T. Sato, K. Haryu, T. Endo and M. Shimada, "High-Temperature Oxidation of Silicon Nitride-based Ceramics by Water Vapour," *J. Mat. Sci.*, **22**, 2635-2640 (1987).

[8]M. Maeda, K. Nakamura and T. Ohkubo, "Oxidation of Silicon Nitride in a Wet Atmosphere," *J. Mater. Sci.*, **24** 2120-26 (1989).

[9]M. Maeda, K. Nakamura and M. Yamada, "Oxidation Resistance of Silicon Nitride Ceramics with Various Additives," *J. Mater. Sci.*, **25** 3790-94 (1990).

[10]D. J. Choi, D. B. Fishbach, and W. D. Scott, "Oxidation of Chemically-Vapor-Deposited Silicon Nitride and Single-Crystal Silicon," *J. Am. Ceram. Soc.*, **72** [7] 1118-1123 (1989).

[11]E. Proverbio, D. Rossi and R. Cigna, "Influence of Water Vapour on High-Temperature Oxidation of Al_2O_3 - MgO-doped Hot-pressed Silicon Nitride," *J. Euro. Ceram. Soc.*, **9** 453-58 (1992).

[12]E. J. Opila, "Oxidation Kinetics of Chemically Vapor-Deposited Silicon Carbide in Wet Oxygen," *J. Am. Ceram. Soc.*, **77** [3] 730-36 (1994).

[13]E. J. Opila and R. E. Hann, "Paralinear Oxidation of CVD SiC in Water Vapor," J. *Am. Ceram. Soc.*, **80** [1] 197-205 (1997).

[14]E. L. Brady, "Chemical Nature of Silica Carried by Steam," *J. Phys. Chem.* **57**, 706 (1953).

[15]A. Hashimoto, "The Effect of H2O Gas on Volatilities of Planet-Forming Major Elements: I. Experimental Determination of Thermodynamic Properties of Ca-, Al-, and Si-Hydroxide Gas Molecules and Its Application to the Solar Nebula," *Geochim. Cosmochim. Acta*, **56**, 511-32 (1992).

[16]D. L. Hildenbrand and K. H. Lau, "Thermochemistry of Gaseous SiO(OH), $SiO(OH)_2$, and SiO_2," *J. Chem. Phys.* **101** [7] 6076-70 (1994).

[17]E. J. Opila, D. S. Fox and N. S. Jacobson, "Mass Spectrometric Identification of $Si(OH)_4$ from the Reaction of Silica with Water Vapor," *J. Am. Ceram. Soc.*, **80** [4] 1009-12 (1997).

[18]C. S. Tedmon, Jr., "The Effect of Oxide Volatilization on the Oxidation Kinetics of Cr and Fe-Cr Alloys," *J. Electrochem. Soc.*, **113** [8] 766-68 (1967).

[19]E. J. Opila and N. S. Jacobson, "SiO(g) Formation from SiC in Mixed Oxidizing-Reducing Gases," *Oxid. Met.*, **44** [5/6] 527-44 (1995).

[20]G. R. Belton and F. D. Richardson, "A Volatile Iron Hydroxide," *Trans. Faraday Soc.*, **50,** 1562-72 (1962).

[21]C. H. Brase and C. P. Brase, *Understandable Statistics, 5th Ed.,* p. 679-681. D. C. Heath and Company, Lexington, KY (1995).

[22]D. M. Mieskowski and W. A. Sanders, "Oxidation of Silicon Nitride Sintered with Rare-Earth Oxide Additions," *J. Am. Ceram. Soc.*, **68** [7] C-160-163 (1985).

[23]M. K. Cinibulk and G. Thomas, "Oxidation Behavior of Rare-Earth Disilicate-Silicon Nitride Ceramics," *J. Am. Ceram. Soc.*, **75** [8] 2044-49 (1992).

[24]H-J. Choi, J-G. Lee and Y-W. Kim, "Oxidation Behavior of Hot-pressed Si_3N_4 with Re_2O_3 (Re = Y, Yb, Er, La)," *J. Euro. Ceram. Soc.*, **19** 2757-62 (1999).

[25]D. S. Fox, "Oxidation Behavior of Chemically-Vapor-Deposited Silicon Carbide and Silicon Nitride from 1200 to 1600°C," *J. Am. Ceram. Soc.*, **81** [4] 945-50 (1998).

[26]E. J. Opila, "Variation of the Oxidation Rate of Silicon Carbide with Water-Vapor Pressure," *J. Am. Ceram. Soc.*, **82**, [3], 625-36 (1999).

[27]B. E. Deal and A. S. Grove, "General Relationship For Thermal Oxidation Of Silicon," *J. Appl. Phys.*, **36** [12] 3770-78 (1965).

[28]E. J. Opila, J. L. Smialek, R. C. Robinson, D. S. Fox, and N. S. Jacobson, "SiC Recession Caused by SiO2 Scale Volatility under Combustion Conditions: II, Thermodynamics and Gaseous-Diffusion Model," *J. Am. Ceram. Soc.*, **82** [7] 1826-34 (1999).

[29]W. M. Kays and M. E. Crawford, *Convective Heat and Mass Transfer*; p. 139. McGraw-Hill, New York, 1980.

[30]O. H. Krikorian, "Thermodynamics of the Silica-Steam System"; p. 481 in *Symposium on Engineering with Nuclear Explosives*, Vol. 1 (Las Vegas, NV, January 14-16, 1970), unpublished.

[31]M. D. Allendorf, C. F. Melius, P. Ho, and M. R. Zachariah, "Theoretical Study of the Thermochemistry of Molecules in the Si-O-H System," *J. Phys. Chem.*, **99** [41] 15285-93 (1995).

[32]J. L. Smialek, R. C. Robinson, E. J. Opila, D. S. Fox and N. S. Jacobson, "SiC and Si_3N_4 Recession Due to SiO_2 Scale Volatility Under Combustor Conditions," *Adv. Composite Mater.*, **8** [1] 33-45 (1999).

[33]R. C. Robinson and J. L. Smialek, "SiC Recession Caused by SiO_2 Scale Volatility under Combustion Conditions: I, Experimental Results and Empirical Model," *J. Am. Ceram. Soc.*, **82** [7] 1817-25 (1999).

Figure captions

Fig. 1. Paralinear kinetics of CVD SiC and linear kinetics of fused quartz at 1200°C in 50% H_2O - 50% O_2 flowing at 4.4 cm/s (adapted from Ref. 13).

Fig. 2. Parabolic kinetics of CVD, SN282 and AS800 Si_3N_4 in 0.44 cm/s dry O_2 at 1300°C.

Fig. 3. Parabolic rate constants (k_p) for AS800 Si_3N_4 at 1200-1400°C in dry oxygen flowing at 0.44 cm/sec

Fig. 4. Surface morphology of silicon nitride after 100 h at 1400°C in dry oxygen: (A) CVD; (B) SN282; (C) AS800.

Fig. 5. Paralinear weight change kinetics for CVD Si_3N_4 at 1200°C in 50% H_2O - 50% O_2 flowing at 4.4 cm/s. The solid line is the result of the least-squares analysis of the data.

Fig. 6. Paralinear weight change kinetics for SN282 Si_3N_4 at 1200°C in 50% H_2O - 50% O_2 flowing at 4.4 cm/s

Fig. 7. Paralinear weight change kinetics for AS800 Si_3N_4 at 1200°C in 50% H_2O - 50% O_2 flowing at 4.4 cm/s.

Fig. 8. Linear rate constants (k_l) for all three Si_3N_4 materials in 50% H_2O - 50% O_2 flowing at 4.4 cm/s.

Fig. 9. Surface morphology of silicon nitride after 100 h at 1400°C, 50% H_2O - 50% O_2: (A) CVD; (B) SN282; (C) AS800.

Fig. 10. Parabolic rate constants (k_p) for the three Si_3N_4 materials in dry oxygen flowing at 0.44 cm/sec

Fig. 11. Comparison of Si_3N_4 weight loss in the GRC high-pressure burner rig under standard fuel-lean conditions: sample temperature ≈ 1200°C; gas velocity = 21 m/s; total pressure = 600 kPa.

Table I. Silicon nitride materials

	CVD Si_3N_4	SN282 Si_3N_4	AS800 Si_3N_4
Manufacturer	Advanced Ceramics Corporation	Kyocera Industrial Ceramics Corporation	AlliedSignal Ceramic Components
Major additives/ impurities	Major - none Minor - C, O ppm - H, Al, Fe	Major – Lu Minor - W, C ppm - Yb, Ca, Mg, Y, Fe, Ba, Mn, Sr	Major - La, Y, Sr Minor – C ppm - Ba, Fe
Density (g/cm^3)	3.18	3.37	3.32
TGA sample size (cm)	2.5 × 0.7 × 0.3	2.6 x 1.3 x 0.3	2.5 × 1.3 × 0.3
Surface area (cm^2)	7.8	9.1	9.0

Major = > 1%, Minor = 0.1 to 1.0%

Table II. Parabolic rate constants (k_p) of Si_3N_4 determined from TGA experiments in dry oxygen at flowing 0.44 cm/s.

Temperature	k_p (mg^2/cm^4 h)		
T (°C)	CVD	SN282	AS800
1200°C	4.1×10^{-6}	8.5×10^{-6}	1.7×10^{-4}
	5.2×10^{-6}	2.0×10^{-5}	2.1×10^{-4}
	6.2×10^{-6}	2.5×10^{-5}	2.2×10^{-4}
	7.0×10^{-6}		2.2×10^{-4}
			2.3×10^{-4}
1300°C	1.2×10^{-5}	3.9×10^{-5}	3.1×10^{-4}
	1.4×10^{-5}	6.0×10^{-5}	3.4×10^{-4}
	2.3×10^{-5}	6.6×10^{-5}	3.4×10^{-4}
			3.8×10^{-4}
1400°C	4.4×10^{-5}	1.3×10^{-4}	6.6×10^{-4}
	5.3×10^{-5}	1.6×10^{-4}	7.8×10^{-4}
	5.9×10^{-5}	7.8×10^{-5}	9.7×10^{-4}
Activation energy (kJ/mol)	227 ± 44	204 ± 79	135 ± 31

Table III. X-ray diffraction characterization of the surface oxide

	Dry oxygen			50% H_2O - 50% O_2		
	1200°C	1300°C	1400°C	1200°C	1300°C	1400°C
CVD	(amorphous)	α-cristobalite	α-cristobalite	(amorphous)	α-cristobalite	α-cristobalite
SN282	α-cristobalite	α-cristobalite	α-cristobalite	α-cristobalite	α-cristobalite	α-cristobalite
	$Lu_2Si_2O_7$	$Lu_2Si_2O_7$	$Lu_2Si_2O_7$	$Lu_2Si_2O_7$	$Lu_2Si_2O_7$	$Lu_2Si_2O_7$
		Lu_2SiO_5*	Lu_2SiO_5*			
AS800	α-cristobalite	α-cristobalite	α-cristobalite	α-cristobalite	α-cristobalite	α-cristobalite
			Y_2O_3*	Y_2O_3*	Y_2O_3*	Y_2O_3*
				$La_2Si_2O_7$*	$La_2Si_2O_7$*	$La_2Si_2O_7$*

*** Not major peaks; provisional identification**

Table IV. Oxide thickness measurements (μm)

	Dry oxygen			50% H_2O - 50% O_2		
	1200°C	1300°C	1400°C	1200°C	1300°C	1400°C
CVD	---	0.69 ± 0.16	1.83 ± 0.65	---	---	3.88 ± 0.88
SN282	---	1.04 ± 0.09	2.39 ± 0.29	---	1.81 ± 0.29	5.51 ± 1.09
AS800	2.92 ± 0.60	4.90 ± 1.51	5.02 ± 1.48	2.99 ± 0.96	5.33 ± 1.89	9.96 ± 2.97

Table V. Parabolic rate constants (k_p) of Si_3N_4 determined from TGA experiments in 50% H_2O - 50% O_2 flowing at 4.4 cm/s.

	k_p (mg^2/cm^4 h)		
T (°C)	CVD	SN282	AS800
1200°C	6.7×10^{-4}	1.4×10^{-4}	1.6×10^{-3}
	9.5×10^{-4}	4.5×10^{-5}	1.8×10^{-3}
1300°C	1.8×10^{-4}	1.4×10^{-4}	7.3×10^{-4}
	5.2×10^{-4}	5.3×10^{-4}	9.8×10^{-4}
		6.0×10^{-4}	
1400°C	1.1×10^{-3}	2.9×10^{-4}	4.5×10^{-2}
	9.3×10^{-4}	6.0×10^{-4}	5.8×10^{-2}
Activation energy (kJ/mol)	20 ± 211	174 ± 200	338 ± 413

Table VI. Si_3N_4 and CVD SiC* linear volatilization rate constants (k_l in mg/cm^2 h) determined from TGA experiments in 50% H_2O/50% O_2 flowing at 4.4 cm/s.

Temperature	CVD Si_3N_4	SN282 Si_3N_4	AS800 Si_3N_4	CVD SiC*
1200°C	4.7×10^{-3}	9.7×10^{-4}	5.1×10^{-3}	5.1×10^{-3}
	5.2×10^{-3}	9.9×10^{-4}	6.7×10^{-3}	5.3×10^{-3}
1300°C	5.3×10^{-3}	1.2×10^{-3}	3.6×10^{-3}	1.6×10^{-3}
	7.7×10^{-3}	2.2×10^{-3}	4.8×10^{-3}	2.7×10^{-3}
		2.5×10^{-3}		5.1×10^{-3}
1400°C	5.5×10^{-3}	1.1×10^{-3}	6.2×10^{-3}	6.4×10^{-3}
	6.8×10^{-3}	2.5×10^{-3}	6.4×10^{-3}	7.8×10^{-3}
			7.1×10^{-3}	
Activation energy	22 ± 51 kJ/mol	55 ± 111 kJ/mol	14 ± 60 kJ/mol	3 ± 75 kJ/mol

*Note: Data for CVD SiC is from Reference 13.

Table VII. Comparison of calculated weight change from SEM cross-section measurements with actual measured weight in 50% H_2O - 50% O_2 flowing at 4.4 cm/s.

Material	Exposure temperature	Time (h)	SEM oxide thickness (μm)	Calculated Δwt (mg/cm^2) from oxide thickness	Measured Δwt (mg/cm^2) from pan balance
CVD	1400°C	100	3.88 ± 0.88	0.200	-0.274
SN282	1300°C	98	1.81 ± 0.29	0.093	+0.029
SN282	1400°C	100	5.51 ± 1.09	0.284	+0.009
AS800	1200°C	100	2.99 ± 0.96	0.154	-0.152
AS800	1300°C	98	5.33 ± 1.89	0.274	+0.006
AS800	1400°C	98	9.96 ± 2.97	0.513	+0.716

Table I. Silicon nitride materials

	CVD Si_3N_4	SN282 Si_3N_4	AS800 Si_3N_4
Manufacturer	Advanced Ceramics Corporation	Kyocera Industrial Ceramics Corporation	AlliedSignal Ceramic Components
Major additives/ impurities	0.5% C, 0.5% O, 0.02% H, 30 ppm Al, 20 ppm Fe	7% Lu, 0.3% W, 0.2%C, 470 ppm Yb, 70 ppm Ca, 20 ppm Mg, 15 ppm Y, 10 ppm Fe, 8 ppm Ba, 2 ppm Mn, 1 ppm Sr	4.2% La, 1.3% Y, 1.0% Sr, 0.06% C, 40 ppm Ba, 30 ppm Fe
Density (g/cm^3)	3.18	3.37	3.32
TGA sample size (cm)	2.5 × 0.7 × 0.3	2.6 x 1.3 x 0.3	2.5 × 1.3 × 0.3
Surface area (cm^2)	7.8	9.1	9.0

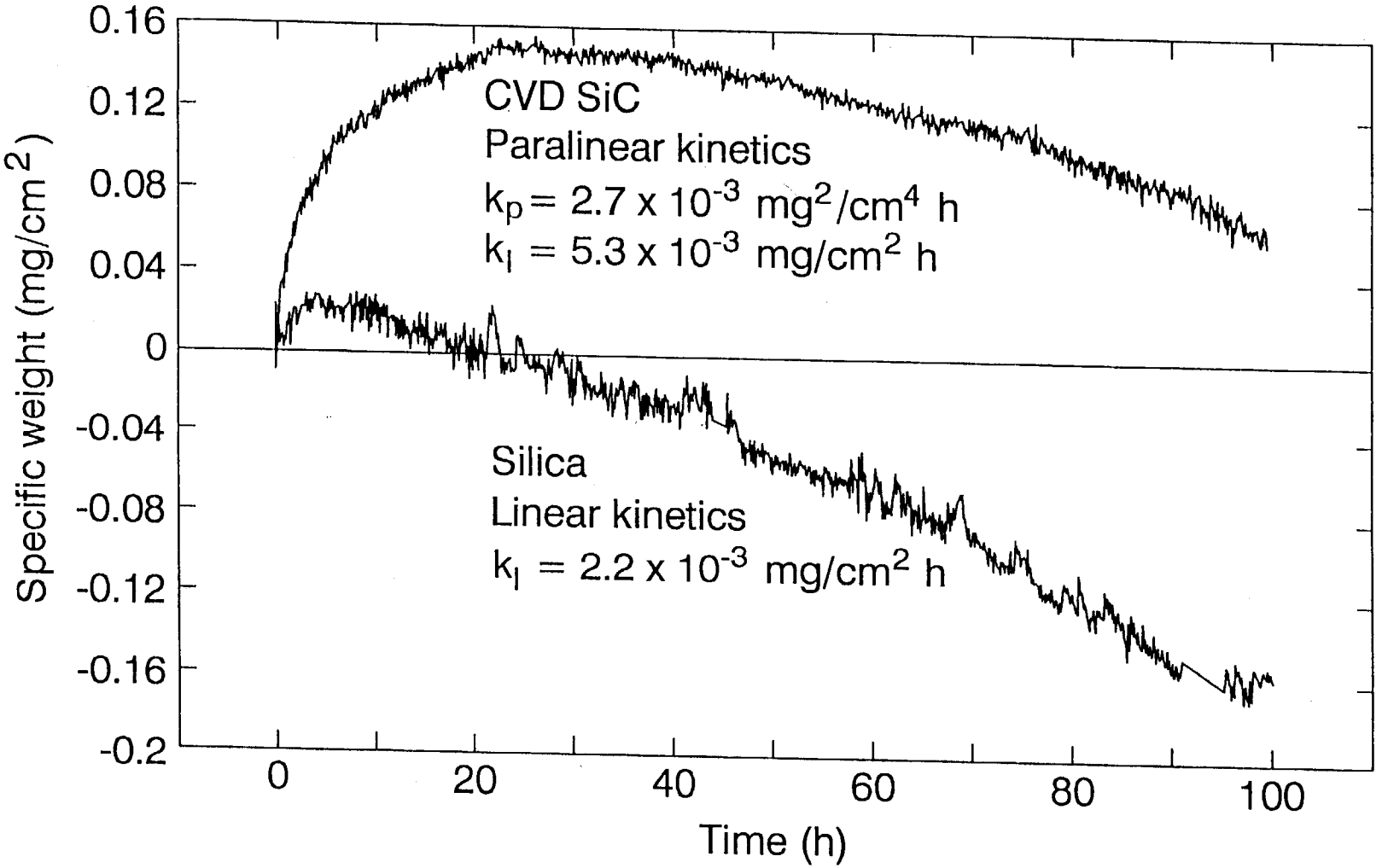

Fig. 1. Paralinear kinetics of CVD SiC and linear kinetics of fused quartz at 1200°C in 50% H_2O - 50% O_2 flowing at 4.4 cm/s (adapted from Ref. 13).

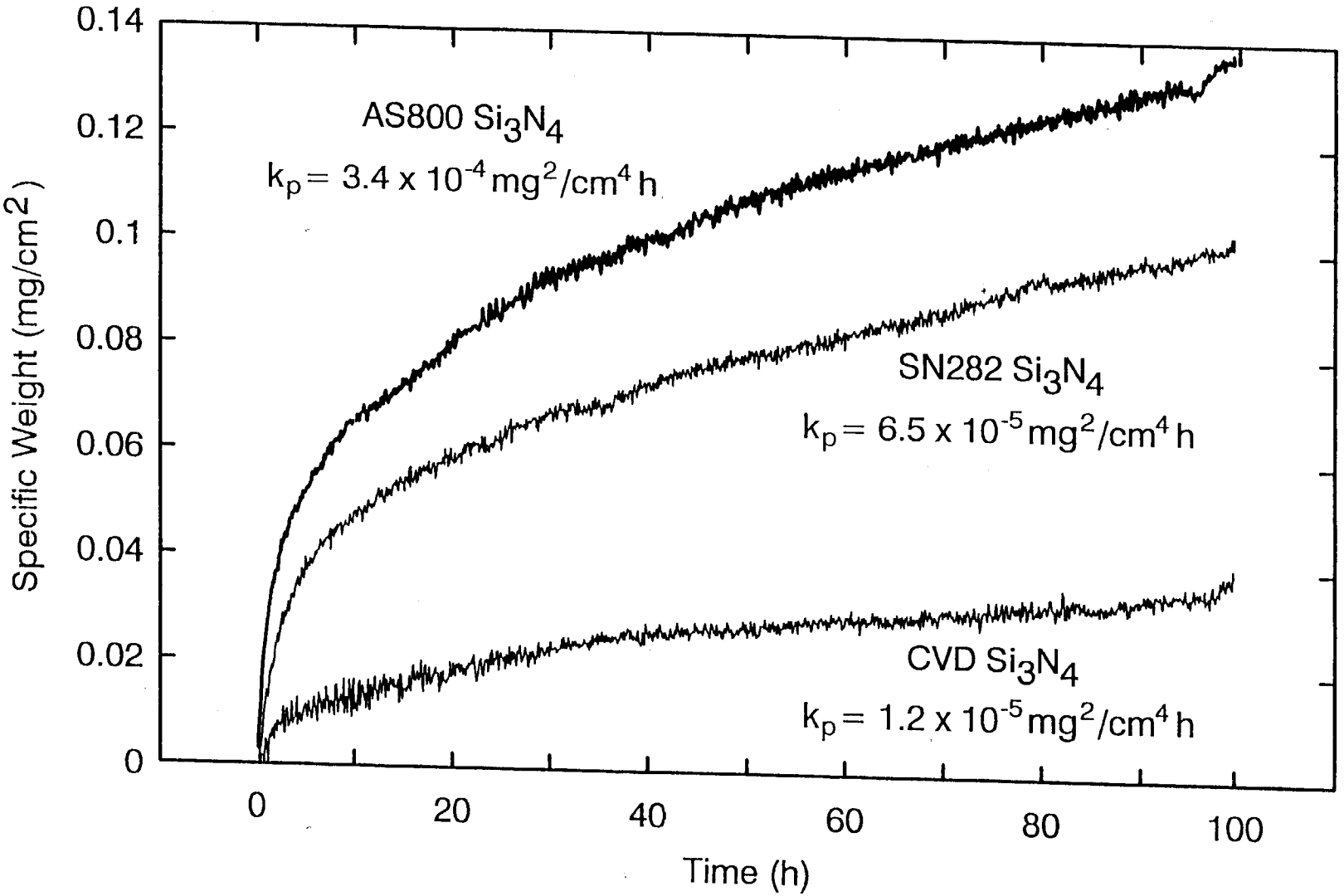

Fig. 2. Parabolic kinetics of CVD, SN282 and AS800 Si_3N_4 in 0.44 cm/s dry O_2 at 1300°C.

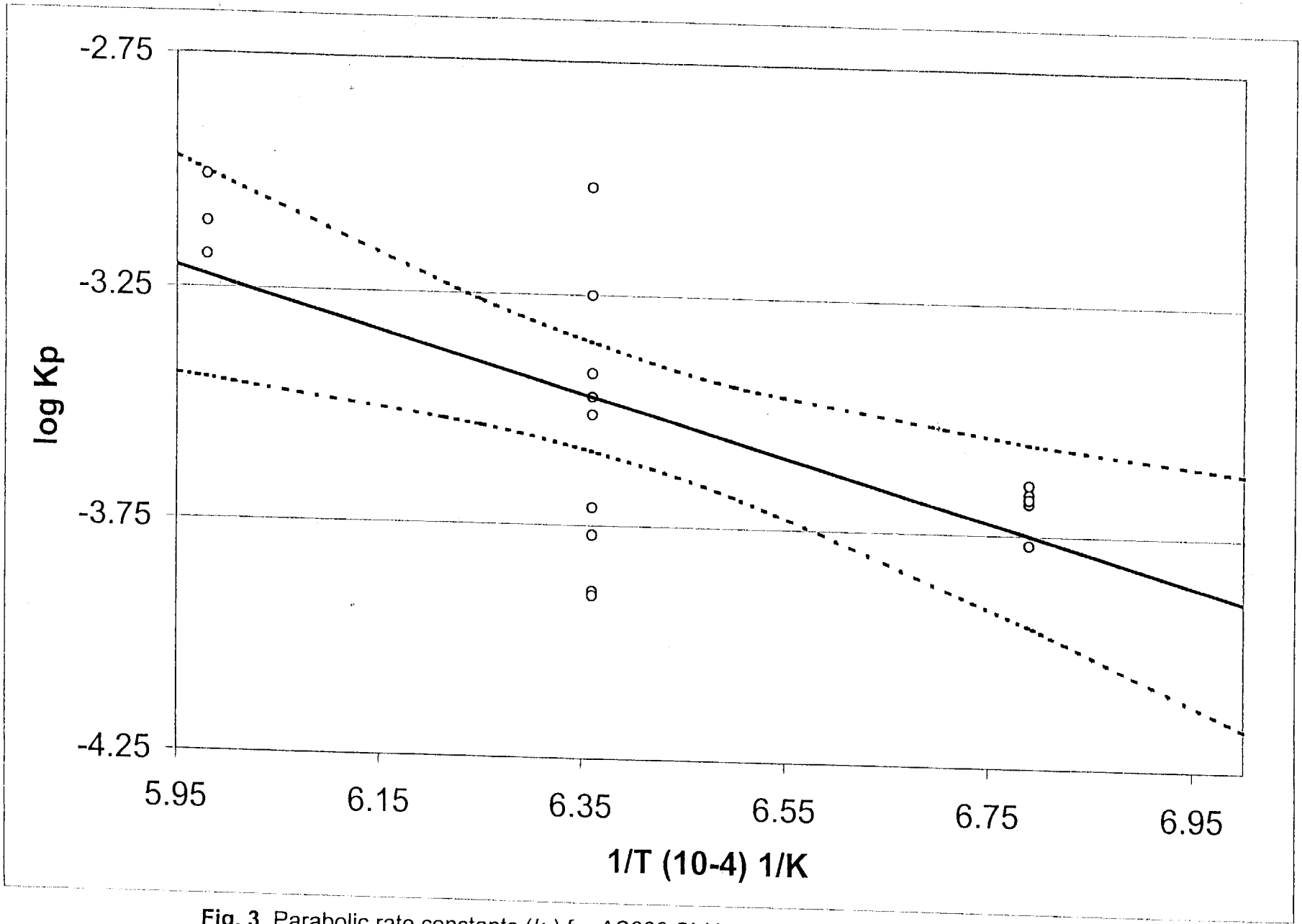

Fig. 3. Parabolic rate constants (k_p) for AS800 Si_3N_4 at 1200-1400°C in dry oxygen flowing at 0.44 cm/sec

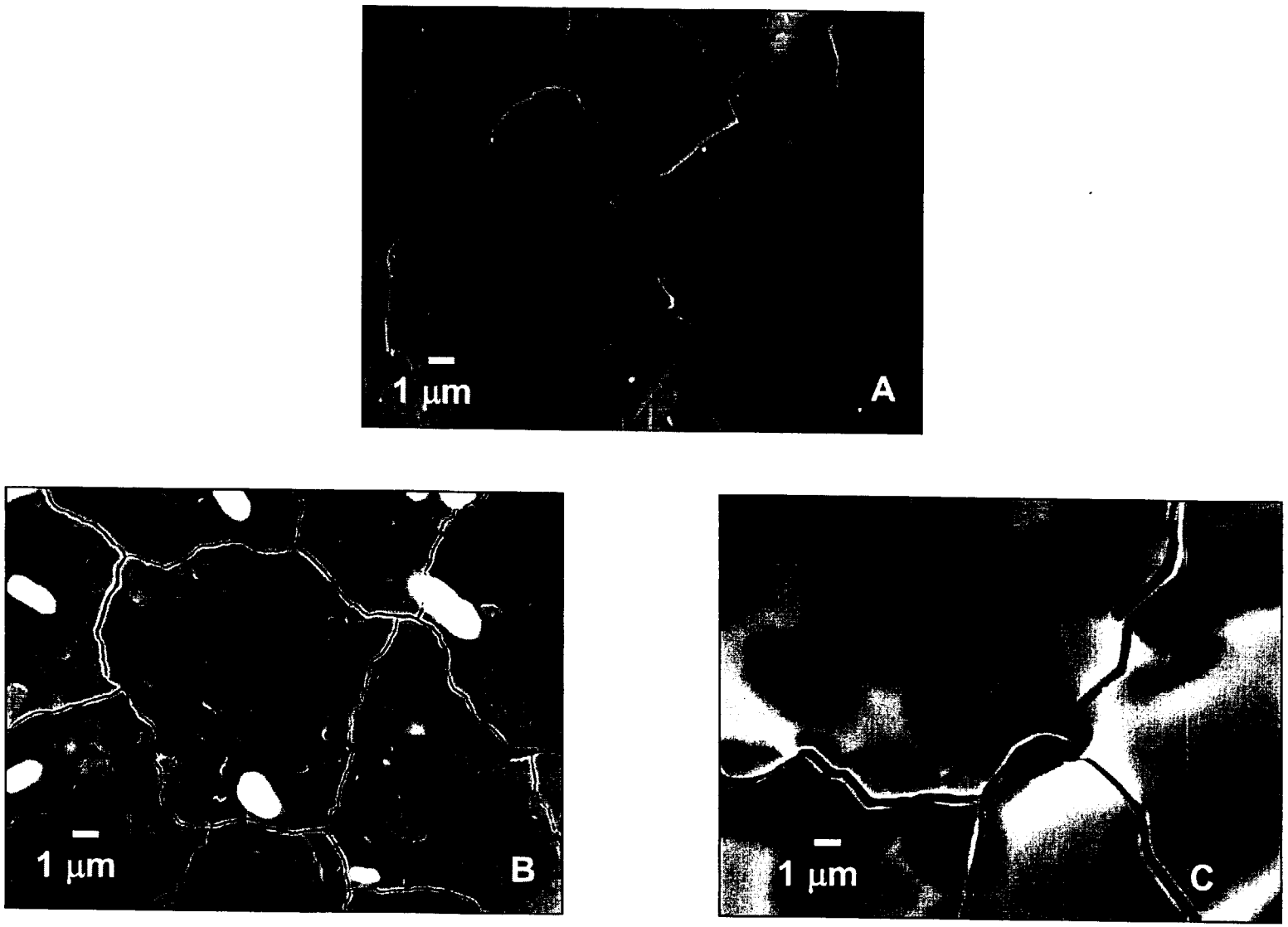

Fig. 4 Surface morphology of silicon nitride after 100 h at 1400 C in dry oxygen: (A)CVD; (B) SN282; (C) AS800.

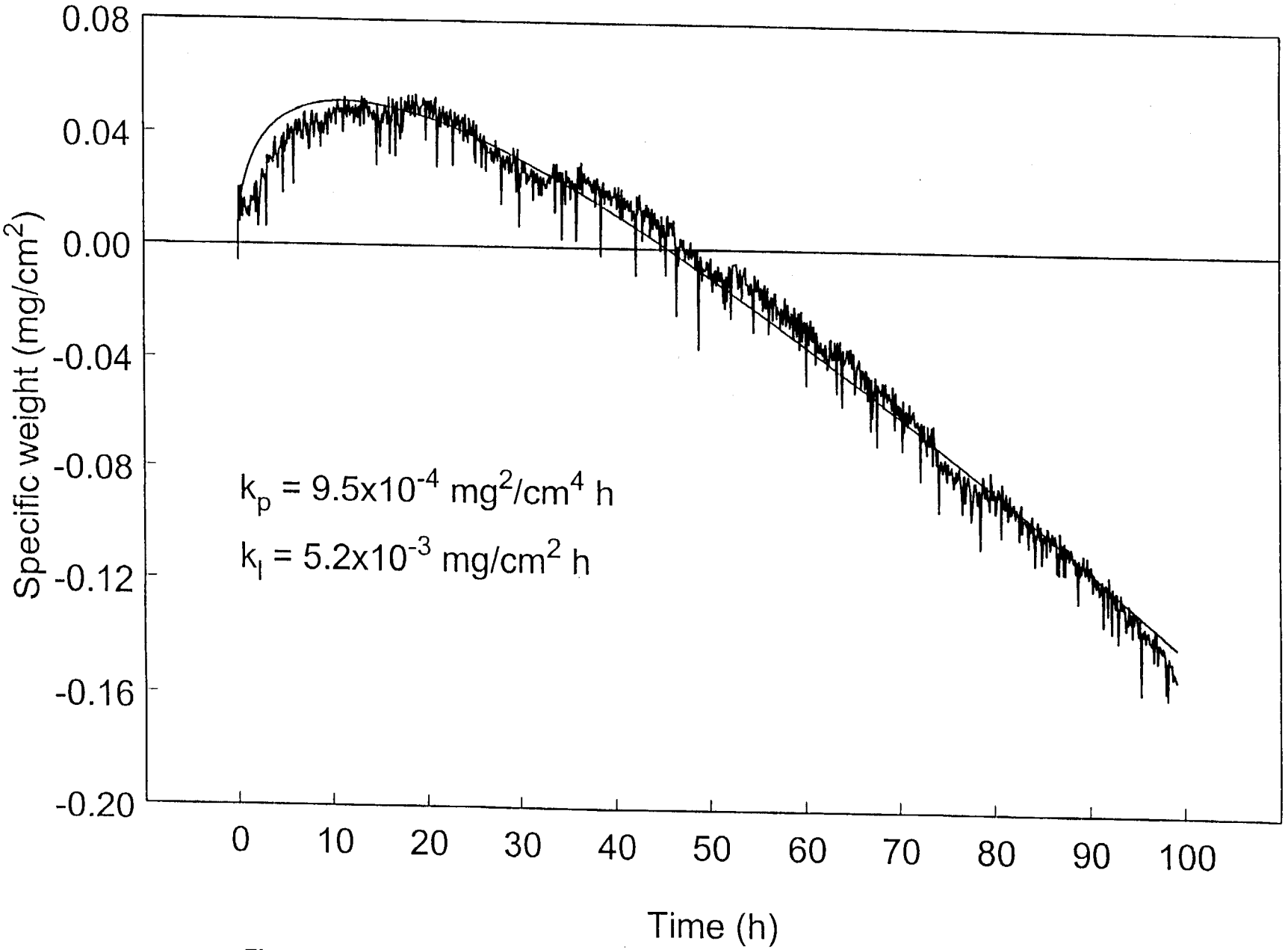

Fig. 5. Paralinear weight change kinetics for CVD Si_3N_4 at 1200°C in 50% H_2O - 50% O_2 flowing at 4.4 cm/s. The solid line is the result of the least-squares analysis of the data.

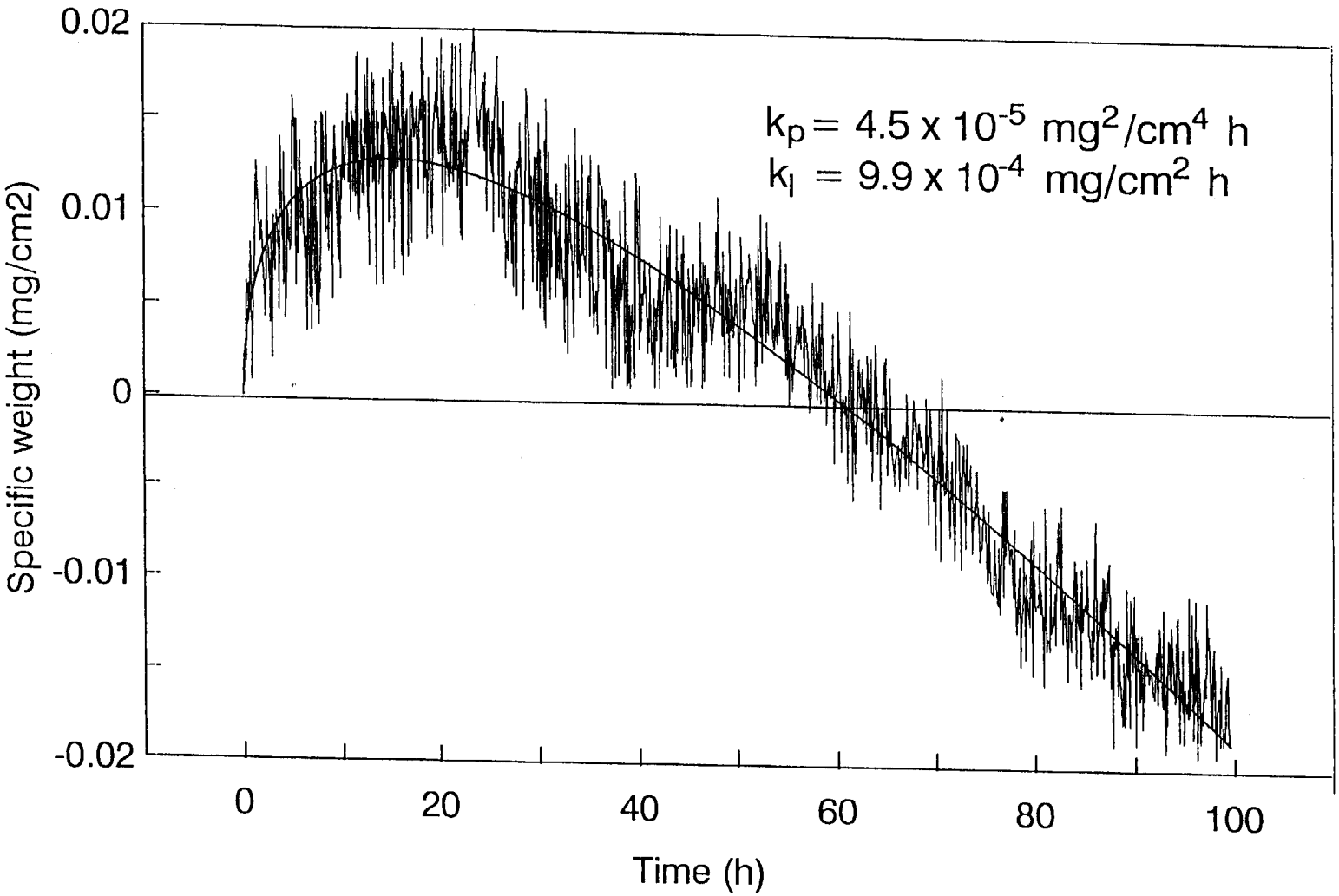

Fig. 6. Paralinear weight change kinetics for SN282 Si_3N_4 at 1200°C in 50% H_2O - 50% O_2 flowing at 4.4 cm/s

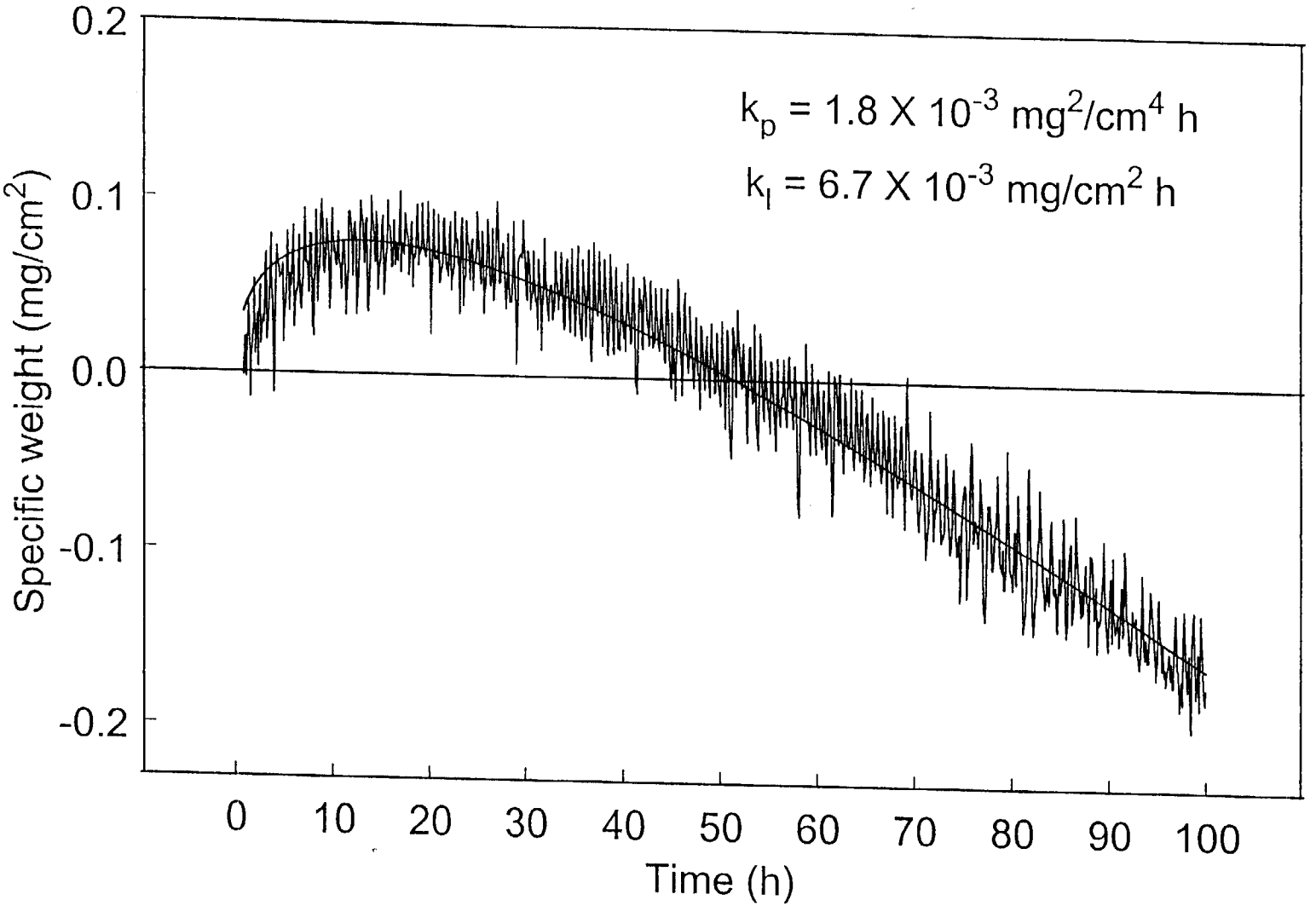

Fig. 7. Paralinear weight change kinetics for AS800 Si_3N_4 at 1200°C in 50% H_2O - 50% O_2 flowing at 4.4 cm/s.

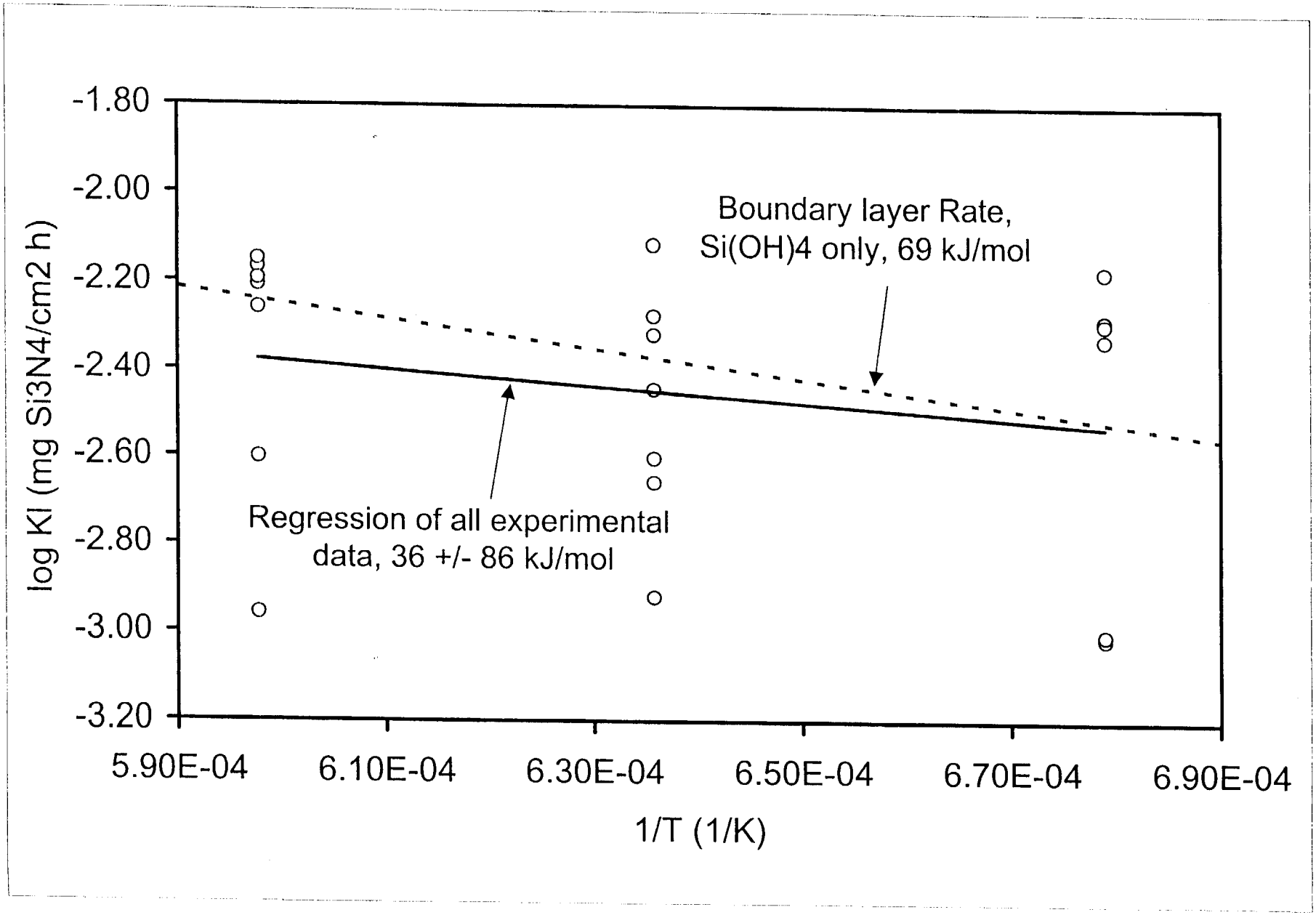

Fig. 8. Linear rate constants (k_l) for all three Si_3N_4 materials in 50% H_2O - 50% O_2 flowing at 4.4 cm/s.

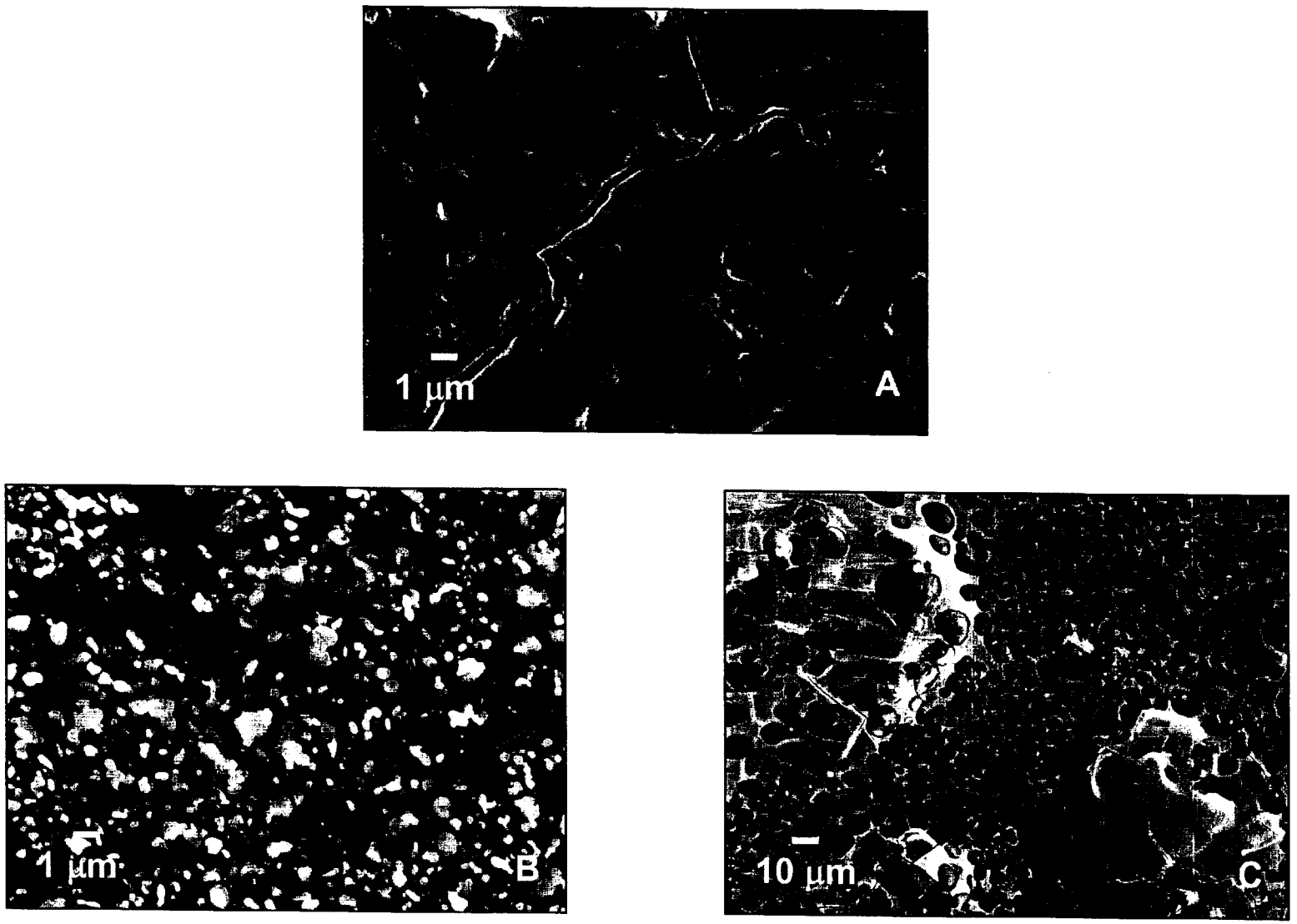

Fig. 9 Surface morphology of silicon nitride after 100 h at 1400 C, 50% water vapor in oxygen: (A)CVD; (B) SN282; (C) AS800.

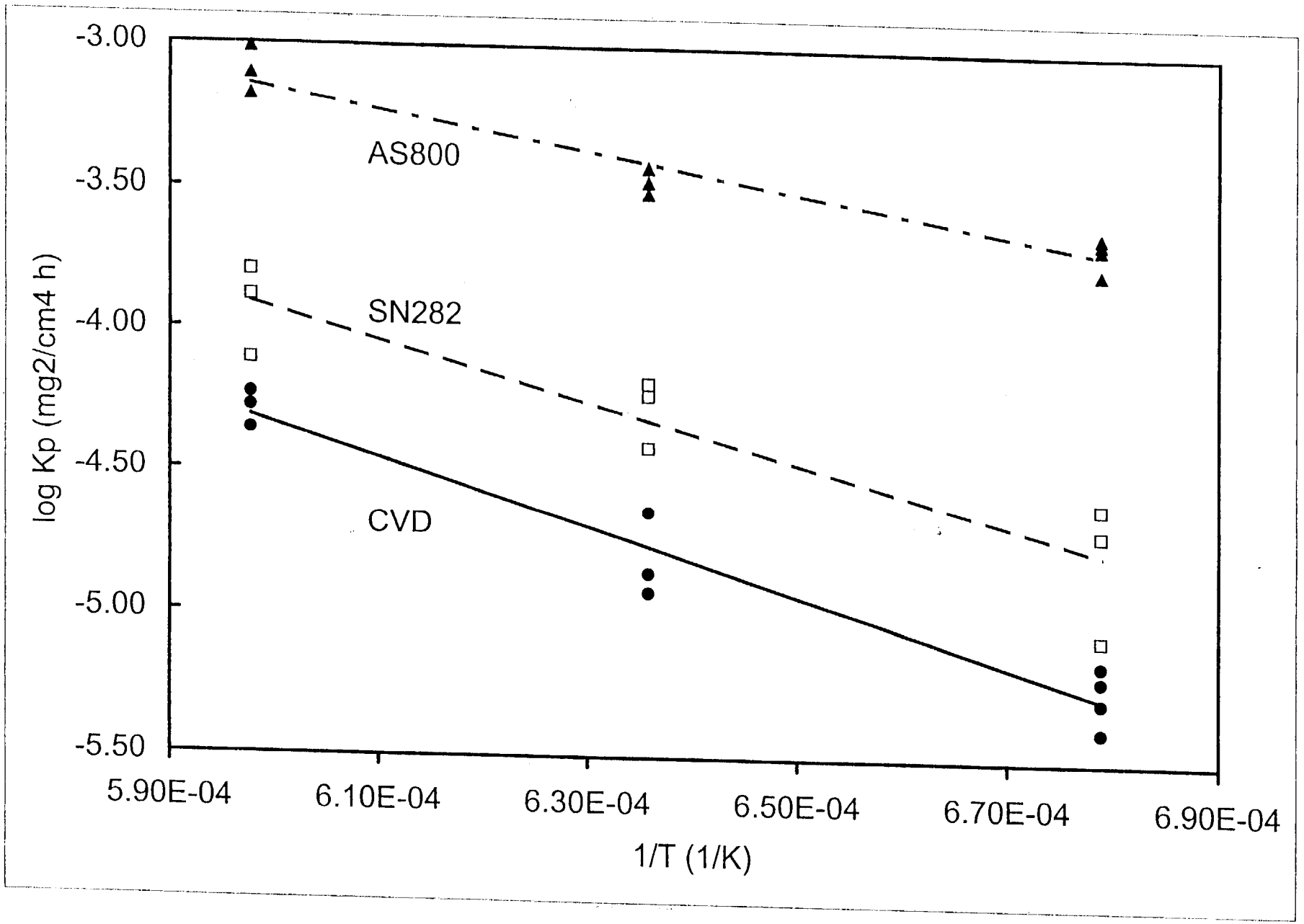

Fig. 10. Parabolic rate constants (k_p) for the three Si_3N_4 materials in dry oxygen flowing at 0.44 cm/sec

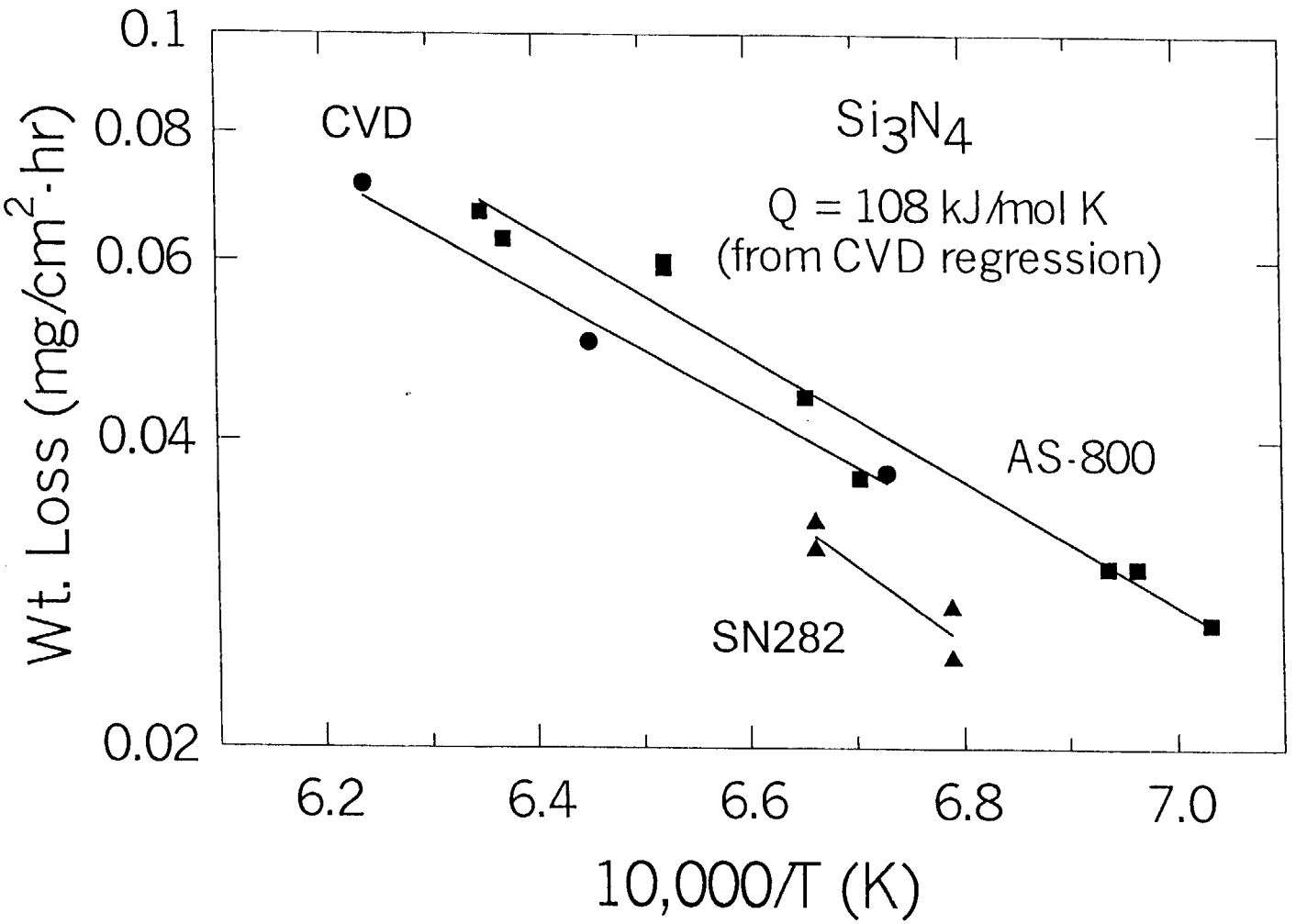

Fig. 11. Comparison of Si_3N_4 weight loss in the GRC high-pressure burner rig under standard fuel-lean conditions: sample temperature ≈ 1200°C; gas velocity = 21 m/s; total pressure = 600 kPa.